Available online at www.sciencedirect.com
SCIENCE DIRECT®
Inorganica Chimica Acta 358 (2005) 4217–4228
Inorganica Chimica Acta
www.elsevier.com/locate/ica

Gold acyls and imidoyls prepared from anionic Fischer-type carbene complexes

Helgard G. Raubenheimer *, Matthias W. Esterhuysen, Catharine Esterhuysen [1]

Department of Chemistry and Polymer Science, University of Stellenbosch, Private Bag X1, Matieland 7602, Stellenbosch, South Africa

Received 26 January 2005; revised 2 March 2005; accepted 14 March 2005
Available online 12 April 2005

Dedicated to Professor Hubert Schmidbaur on the occasion of his 70th birthday.

Abstract

Reaction of $[(CO)_5WC(O)Ph]Li$ or $[(CO)_5WC(O)Ph]NBu_4$ with Ph_3PAuCl affords acyl complexes of gold. In the latter conversion, both the crystalline products $[(CO)_5WCl]NBu_4$ (**2**) and $Ph_3PAuC(O)Ph$ (**3**) have been isolated and fully characterised. Similarly, imidoyl gold compounds (**4**–**8**) result from deprotonated aminocarbene complexes, $[(CO)_5MC(NR^2)R^1]Li$ (M = Cr, W; R^1 = Ph, Me; R^2 = H, Me) and Ph_3PAuCl. Crystal and molecular structure determinations of dinuclear $[Ph_3PAuC(NH)Ph] \cdot Cr(CO)_5$ (**6**) show N-coordination of the chromium carbonyl unit that selectively affords a *Z*-isomer.

Keywords: Carbene complexes; Acyl and imidoyl gold complexes; Organometallic synthons; Chloro(pentacarbonyl)tungstate; Gold–gold interactions

1. Introduction

Transition metal–acyl complexes comprise an extremely important class of organometallic compounds. It has long been known that metal–acyl complexes are a ubiquitous feature in many homogenous catalytic processes, especially ones in which carbon monoxide is involved [1], and have hence been the subject of many reactivity and theoretical studies [2]. Transition metal–acyl complexes are also useful models for key catalytic intermediates in heterogeneous catalytic processes [3], such as the Fischer–Tropsch process operated by SASOL, where Fe-surface alkyl and acyl species are believed to play an important role in the formation of oxygenates (mainly formates, alcohols and ketones) [4]. Furthermore, anionic transition metal–acyl complexes are also important intermediates in many synthetic routes to useful organometallic compounds, including Fischer's classical, and Semmelhack's more recent, routes to carbene complexes. Both these routes involve the formation of anionic metal–acyl species that, upon oxygen alkylation, yield a wide variety of carbene complexes [5,6]. Due to the electronic properties of low-valent metal centres in neutral metal–acyl complexes, the acyl moiety is viewed as a close relative of ketones or esters. This analogy has been utilised successfully in developing much of the chemistry of metal–acyl complexes, especially reduction and alkylation reactions [7].

Transition metal–acyl complexes are mostly prepared via three main reaction pathways: the attack by nucleophilic carbon reagents at metal-bound CO; acylation at a nucleophilic metal centre; and the migratory insertion reaction of a CO ligand into an M–C bond [1,8]. From a catalysis point of view the latter, also frequently referred to as catalytic carbonylation, is the more interesting

* Corresponding author. Tel.: +27 21 808 3850; fax: +27 21 808 3849.
E-mail addresses: hgr@sun.ac.za (H.G. Raubenheimer), ce@sun.ac.za (C. Esterhuysen).
[1] Tel.: +27118083345; fax: +27118083360.

0020-1693/$ - see front matter © 2005 Elsevier B.V. All rights reserved.
doi:10.1016/j.ica.2005.03.029

route. This route provides a mechanism for the incorporation of CO feedstock into organic compounds and polymers (mostly co-polymers with ethylene) and is indeed unequalled in importance in catalytic conversions involving CO. This transformation has many practical applications and a great number of catalytic carbonylations are employed in both laboratory and industrial syntheses [1]. The relationship between anionic carbene complexes and acyl complexes of Group 6 metals is shown in Scheme 1.

There are no reports in the literature of simple insertion reactions of CO into Au–C bonds. It has, however, been observed that Au–C(O)OR derivatives can be obtained from reactions of gold(III) complexes under conditions where alkoxy (OR) complexes may be expected as intermediates [9].

From the above-mentioned considerations, it becomes clear that the synthesis of gold–acyl complexes along conventional reaction pathways is not possible. We have reported previously [10] that alkoxycarbene complexes deprotonated α to the carbene carbon react with Ph_3PAu^+ (a fragment isolobal to H^+) by transmetallation and 'aurolysis' (a second formal metal exchange), to form alkoxyvinylgold compounds. Herein, the C(carbene)–CH_2 connectivity appears largely as a double bond coordinated to expelled $Cr(CO)_5$ (Eq. (1)).

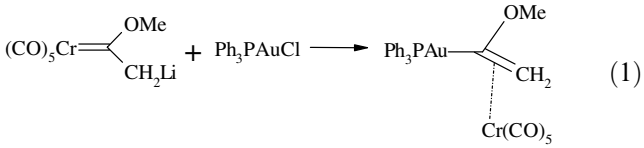

(1)

The question we address in the present work is whether it is possible to similarly express the C(O)R and $C(NR^2)R^1$ double bonds in *untrapped* acyl and imidoyl complexes of gold by using deprotonated hydroxycarbene (that is acylate – compare Scheme 1) and aminocarbene (imidoylate) complexes of group 6 metals as starting materials. Haupt recently successfully trapped the first acylgold(I) complexes along a similar synthetic pathway as O-coordinated, axial ligands to $Re_2(\mu\text{-}PPh_2)(CO)_7$ fragments; the uncoordinated gold–acyl species, however, remained elusive [11].

Previous work in our laboratory not only involved the isolation and characterisation of anionic acylate complexes [12], but also their utilisation as O-donor ligands towards harder metals such as Zr(IV) for catalytic application [13].

Although many interesting imidoyl complexes of gold have been reported, all of these involve imine groups that are either situated in heterocyclic ring systems [14] or contain heteroatoms (O or N) bonded to the α-carbon atom [15].

Herein, we report the first successful method for the isolation of unattached gold acyl complex systems as well as a simple, related protocol for the preparation of imidoylgold(I) compounds.

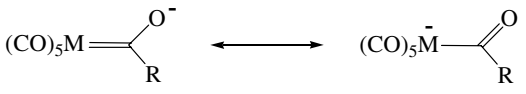

Scheme 1.

2. Experimental

2.1. General procedures and instruments

All solvents were dried and purified by conventional methods and freshly distilled under nitrogen shortly before use. Unless otherwise stated, all common reagents were used as obtained from commercial suppliers without further purification. PhLi was freshly prepared by the reaction of metallic Li with bromobenzene in Et_2O. MeLi, PhLi and BuLi were standardised before use according to the procedure reported by Winkle et al. [16]. Ph_3PAuCl [17], the tetrabutylammonium acetyl/benzoylpentacarbonyl chromates and tungstates [18], and the group 6 metal pentacarbonyl Fischer-type aminocarbene starting complexes [19] were prepared according to the procedures described in the literature. All reactions and manipulations involving organometallic reagents were carried out under a dry nitrogen atmosphere using standard Schlenk and vacuum-line techniques. NMR spectra were recorded on Varian INOVA 600 (600 MHz for ^1H, 151 MHz for $^{13}C\{^1H\}$ and 243 MHz for $^{31}P\{^1H\}$) or Varian VXR 300 (300 MHz for ^1H, 75.4 MHz for $^{13}C\{^1H\}$ and 121.5 MHz for $^{31}P\{^1H\}$) NMR spectrometers. ^1H and ^{13}C chemical shifts are reported in ppm relative to the ^1H and ^{13}C residue of the deuterated solvents. ^{31}P chemical shifts are reported in ppm relative to an 85% H_3PO_4 external standard solution. IR spectra (4000–400 cm^{-1}, resolution 4 cm^{-1}) were recorded on a Perkin–Elmer 1600 series FTIR spectrometer. FAB-MS were recorded on a Micromass DG 70/70E mass spectrometer using xenon gas as bombardment atoms and *m*-nitrobenzylalcohol as matrix. Flash column chromatography was performed with "flash grade" silica (SDS 230–400 mesh). Crystal structure data collections were carried out on a Nonius KappaCCD diffractometer. Elemental analyses were carried out at the Chemistry department, University of Cape Town.

2.2. Preparation of *1*

1.2 mol equiv. of standardised PhLi was added dropwise to 0.80 mmol (282 mg) $W(CO)_6$ suspended in 20 ml Et_2O at room temperature over a period of 10–15 min. After addition of the PhLi, the mixture was stirred at room temperature for 30 min, after which it was cooled

to −78 °C. $AuPPh_3Cl$ (0.80 mmol; 395 mg) was then added to the cooled reaction mixture. After stirring at −78 °C for 30–45 min, the reaction mixture was allowed to warm to room temperature over a period of $2\frac{1}{2}$ h, during which time the $AuPPh_3Cl$ dissolves and a white LiCl precipitate forms. The mother liquor of the product mixture was carefully removed with a syringe upon settling of the LiCl precipitate. Carefully cooling the mother liquor upon removal of the solvent in vacuo resulted in the formation of crystals of **1** in moderate yield [65%]. The yield was not optimised.

Complex **1**: orange microcrystalline material, yield 839 mg, 65%. IR (KBr, cm^{-1}): *v* 1560 m, 1870 st, 1917 st, 1940 v st, 1972 m, 2065 w. FAB-MS, *m/z* (relative intensity) for $C_{59}H_{50}O_8BrLiP_2Au_2W$: 721 ($(Ph_3P)_2Au^+$, 70), 565 (benzoyl-$AuPPh_3^+$, 25), 459 ($Ph_3PAu^+$, 100), 290 (W(CO)–Br, 10), 263 (W–Br, 15). ^1H NMR (CD_2Cl_2, δ): 7.2–7.6 (m, 18H, Ph), 8.04 (d, $^3J_{H-H}$ = 7.2 Hz, 2H, $PhC_{benzoyl}$). ^{13}C NMR (CD_2Cl_2, δ): 203.3 (br, s, C=O), 199.5 (s, CO_{trans}), 192.1 (s, CO_{cis}), 146.9(s, $PhC_{benzoyl}$), 134.6 (d, $^3J_{P-C}$ = 13.1 Hz, $PPhC_{meta}$), 131.9 (s, $PPhC_{para}$), 131.2 (d, $^1J_{P-C}$ = 53.0 Hz, $PPhC_{ipso}$), 130.7 (s, $PhC_{benzoyl}$), 129.6 (d, $^2J_{P-C}$ = 11.1 Hz, $PPhC_{ortho}$), 127.9 (s, $PhC_{benzoyl}$), 126.1 (s, $PhC_{benzoyl}$). ^{31}P NMR (CD_2Cl_2, δ): 39.8 (s). *Anal.* Calc. for $C_{59}H_{50}O_8BrLiP_2Au_2W$: C, 43.92; H, 3.12; P, 3.84. Found: C, 43.52; H, 2.98; P, 3.95%.

2.3. Preparation of 2 and 3

Complexes **2** and **3** were prepared in much the same way, except that 0.80 mmol Bu_4N benzoylpentacarbonyl tungstate, prepared and isolated separately, was employed in this reaction instead of the freshly prepared lithium benzoylpentacarbonyl tungstate used previously. Instead of a LiCl precipitate forming in the reaction mixture upon completion of the conversion, a precipitate of **3** forms, which is isolated in near quantitative yield (96%) by careful removal of the cooled (−20 °C) mother liquor, now containing only **2**, with a syringe. The isolated precipitate of **3** can be washed with cooled 10 ml portions of Et_2O to remove any remaining traces of **2** if so required. **2** was isolated in high yield (72%) by prolonged crystallisation (~10 weeks) at −20 °C from concentrated Et_2O solutions, prepared directly from the mother liquor. Yields were not optimised.

Complex **2**: orange crystals, yield 325 mg, 72%. IR (KBr, cm^{-1}): *v* 1606 m. FAB-MS, *m/z* (relative intensity) for $C_{25}H_{20}OPAu$: 721 ($(Ph_3P)_2Au^+$, 75), 564 (M^+, 10), 459 (Ph_3PAu^+, 100). ^1H NMR (CD_2Cl_2, δ): 7.91 (d, $^3J_{H-H}$ = 7.2 Hz, 2H $Ph_{benzoyl}C_{ortho}$), 7.2–7.6 (m, 18H, Ph). ^{13}C NMR (CD_2Cl_2, δ): 198.1 (d, $^2J_{P-C}$ = 6.0 Hz, C=O), 140.1 (s, $PhC_{benzoyl}$), 134.6 (d, $^3J_{P-C}$ = 13.1 Hz, $PPhC_{meta}$), 132.2 (s, $PhC_{benzoyl}$), 131.9 (s, $PPhC_{para}$), 131.2 (d, $^1J_{P-C}$ = 53.0 Hz, $PPhC_{ipso}$), 130.1 (s, $PhC_{benzoyl}$), 129.6 (d, $^2J_{P-C}$ = 11.1 Hz, $PPhC_{ortho}$), 128.8 (s, $PhC_{benzoyl}$). ^{31}P NMR (CD_2Cl_2, δ): 37.9 (s). *Anal.* Calc. for $C_{25}H_{20}OPAu$: C, 53.21; H, 3.57; P, 5.49. Found: C, 53.27; H, 3.61; P, 5.50%.

Complex **3**: yellow crystals, yield 462 mg, 96%. Physical and spectroscopic data agree with those reported previously [25].

2.4. Preparation of 4–8

0.4 ml of 1.6 M BuLi (1 mol equiv.) was added to a solution of the Fischer-type aminocarbene complex (0.80 mmol) in 15 ml thf cooled to −78 °C. The mixture was stirred at that temperature for 10 min, after which 1 mol equiv. Ph_3PAuCl (395 mg) was added to the solution. After stirring this mixture at −78 °C for 30 min, it was allowed to warm to room temperature over a period of 21/2 h. Removal of the solvent in vacuo resulted in dark yellow to brown oily residues containing a mixture of products (TLC). The desired products were isolated in moderately low to high yields [32% (**4**), 41% (**5**), 56% (**6**), 85% (**7**) and 57% (**8**)] as broad yellow bands by means of low temperature (−15 °C) silica gel column chromatography (hexane/diethyl ether, 2:1). Yields were not optimised.

Complex **4**: yellow oil, yield 178 mg, 32%. IR (pentane, cm^{-1}): *v* 1902 st, 1929 v st, 1950 w, 2060 w. FAB-MS, *m/z* (relative intensity) for $C_{25}H_{19}NO_5PAuCr$: 721 ($(Ph_3P)_2Au^+$, 70), 459 (Ph_3PAu^+, 100), 694 (M^+, 55). ^1H NMR ($CDCl_3$, δ): 8.89 (br s, 1H, NH), 7.4–7.7 (m, 15H, Ph), 2.28 (s, 3H, CH_3). ^{13}C NMR ($CDCl_3$, δ): 239.6 (d, $^2J_{P-C}$ = 122.1 Hz, NC), 221.8 (s, CO_{trans}), 216.6 (s, CO_{cis}), 134.6 (d, $^3J_{P-C}$ = 13.1 Hz, PhC_{meta}), 132.0 (br s, PhC_{para}), 130.3 (d, $^1J_{P-C}$ = 51.4 Hz, PhC_{ipso}), 129.6 (d, $^2J_{P-C}$ = 11.0 Hz, PhC_{ortho}), 42.1 (br s, CH_3). ^{31}P NMR ($CDCl_3$, δ): 41.9 (s). *Anal.* Calc. for $C_{25}H_{19}NO_5PAuCr$: C, 43.31; H, 2.76; N, 2.02. Found: C, 43.12; H, 2.61; N, 2.15%.

Complex **5**: yellow oil, yield 232 mg, 41%. IR (pentane, cm^{-1}): *v* 1904 st, 1931 v st br, 1953 w, 2058 w. FAB-MS, *m/z* (relative intensity) for $C_{26}H_{21}NO_5PAuCr$: 721 ($(Ph_3P)_2Au^+$, 65), 459 (Ph_3PAu^+, 100). ^1H NMR (CD_2Cl_2, δ): 7.4–7.7 (m, 15H, Ph), 3.24 (s, 3H, NCH_3), 2.25 (s, 3H, CH_3). ^{13}C NMR (CD_2Cl_2, δ): 236.8 (d, $^2J_{P-C}$ = 129.8 Hz, NC), 221.8 (s, CO_{trans}), 216.0 (s, CO_{cis}), 134.6 (d, $^3J_{P-C}$ = 13.4 Hz, PhC_{meta}), 131.9 (s, PhC_{para}), 130.6 (d, $^1J_{P-C}$ = 52.8 Hz, PhC_{ipso}), 129.5 (d, $^2J_{P-C}$ = 11.0 Hz, PhC_{ortho}), 49.4 (d, $^3J_{P-C}$ = 9.3 Hz, CH_3), 32.0 (s, NCH_3). ^{31}P NMR (CD_2Cl_2, δ): 41.9 (s). *Anal.* Calc. for $C_{26}H_{21}NO_5PAuCr$: C, 44.15; H, 2.99; N, 1.98. Found: C, 44.01; H, 3.05; N, 1.96%.

Complex **6**: dark yellow oil, yield 338 mg, 56%. IR (pentane, cm^{-1}): *v* 1904 st, 1930 v st br, 1951 w, 2058 w. FAB-MS, *m/z* (relative intensity) for $C_{30}H_{21}NO_5PAuCr$: 721 ($(Ph_3P)_2Au^+$, 55), 694 (M^+, 100), 459 (Ph_3PAu^+, 80). ^1H NMR (CD_2Cl_2, δ): 9.59 (br s, 1H,

NH), 7.3–7.7 (m, 20H, Ph). ^{13}C NMR (CD_2Cl_2, δ): 232.4 (d, $^2J_{P-C}$ = 131.9 Hz, NC), 221.6 (s, CO_{trans}), 216.1 (s, CO_{cis}), 149.1 (br, s, PhC_{ipso}), 134.5 (d, $^3J_{P-C}$ = 13.4 Hz, $PPhC_{meta}$), 131.9 (s, $PPhC_{para}$), 130.9 (s, $PhC_{o/m/p}$), 130.2 (d, $^1J_{P-C}$ = 51.2 Hz, $PPhC_{ipso}$), 129.5 (d, $^2J_{P-C}$ = 11.0 Hz, $PPhC_{ortho}$), 129.0 (s, $PhC_{o/m/p}$), 126.2 (s, $PhC_{o/m/p}$). ^{31}P NMR (CD_2Cl_2, δ): 42.3 (s). *Anal.* Calc. for $C_{30}H_{21}NO_5PAuCr$: C, 47.70; H, 2.80; N, 1.85. Found: C, 47.65; H, 2.76; N, 2.01%.

Complex **7**: yellow oil, yield 603 mg, 85%. IR (pentane, cm^{-1}): *v* 1904 st, 1924 v st br, 1962 w, 2062 w. FAB-MS, *m/z* (relative intensity) for $C_{30}H_{21}NO_5PAuW$: 830 (M-2CO, 35), 721 ($(Ph_3P)_2Au^+$, 70), 459 (Ph_3PAu^+, 100). ^{1}H NMR (CD_2Cl_2, δ): 10.05 (br s, 1H, NH), 7.4–7.7 (m, 20H, Ph). ^{13}C NMR (CD_2Cl_2, δ): 238.4 (br s, NC), 203.3 (s, CO_{trans}), 199.6 (s, CO_{cis}), 149.4 (br, s, PhC_{ipso}), 134.3 (d, $^3J_{P-C}$ = 10.3 Hz, $PPhC_{meta}$), 132.0 (s, $PPhC_{para}$), 131.3 (s, $PhC_{o/m/p}$), 130.1 (d, $^1J_{P-C}$ = 54.3 Hz, $PPhC_{ipso}$) 129.4 (d, $^2J_{P-C}$ = 9.1 Hz, $PPhC_{ortho}$), 129.3 (s, $PhC_{o/m/p}$), 126.5 (s, $PhC_{o/m/p}$). ^{31}P NMR (CD_2Cl_2, δ): 41.2 (s). *Anal.* Calc. for $C_{30}H_{21}NO_5PAuW$: C, 40.61; H, 2.39; N, 1.58. Found: C, 40.54; H, 2.46; N, 1.65%.

Complex **8**: yellow oil, yield 411 mg, 57%. IR (pentane, cm^{-1}): *v* 1905 st, 1926 v st br, 1964 w, 2064 w. FAB-MS, *m/z* (relative intensity) for $C_{31}H_{23}NO_5PAuW$: 721 ($(Ph_3P)_2Au^+$, 75), 459 (Ph_3PAu^+, 100). ^{1}H NMR ($CDCl_3$, δ): 7.4–7.7 (m, 20H, Ph), 3.34 (s, 3H, NCH_3). ^{13}C NMR ($CDCl_3$, δ): 235.9 (d, $^2J_{P-C}$ = 124.6 Hz, NC), 203.6 (s, CO_{trans}), 199.8 (s, CO_{cis}), 148.8 (br, s, PhC_{ipso}), 134.1 (d, $^3J_{P-C}$ = 10.5 Hz, $PPhC_{meta}$), 131.8 (s, $PPhC_{para}$), 132.0 (s, $PhC_{o/m/p}$), 130.0 (d, $^1J_{P-C}$ = 53.2 Hz, $PPhC_{ipso}$) 129.2 (d, $^2J_{P-C}$ = 9.0 Hz, $PPhC_{ortho}$), 129.1 (s, $PhC_{o/m/p}$), 125.8 (s, $PhC_{o/m/p}$), 32.4 (s, NCH_3). ^{31}P NMR ($CDCl_3$, δ): 39.3 (s). *Anal.* Calc. for $C_{31}H_{23}NO_5PAuW$: C, 41.31; H, 2.57; N, 1.55. Found: C, 41.41; H, 2.59; N, 1.60%.

2.5. X-ray structure determinations

The crystal data collection and refinement details for complexes **1**, **2**, **3** and **6** are summarised in Table 1. X-ray quality orange prismatic single crystals of **1** were obtained by crystallisation of the cooled reaction mixture. Orange platelet crystals of **2**, suitable for X-ray diffraction, were obtained by prolonged crystallisation (~10 weeks) from a concentrated thf solution layered with Et_2O and cooled to −20 °C. Good quality crystals of **3** (yellow platelets) were obtained overnight by recrystallisation of the isolated compounds from a thf solution layered with pentane and cooled to −20 °C. X-ray quality crystals (yellow needles) of **6** were only obtained after an extended period (2 months) of crystallisa-

Table 1
Crystal data and structure refinements for **1**, **2**, **3** and **6**

Compound	**1**	**2**	**3**	**6**
Chemical formula	$C_{59}H_{50}O_8BrLiP_2Au_2W$	$C_{25}H_{20}OPAu$	$C_{21}H_{36}O_5NClW$	$C_{30}H_{21}O_5NPAuCr$
MW (g/mol)	1613.61	564.37	601.81	755.43
Crystal system	monoclinic	monoclinic	monoclinic	orthorhombic
Space group	$P2_1/n$	$P2_1/n$	$C2/c$	$Pc2_1b$
Unit cell dimensions				
a (Å)	15.4626(3)	12.8710(3)	15.7654(2)	11.0724(2)
b (Å)	19.2859(5)	10.3025(3)	19.5093(2)	12.6013(2)
c (Å)	19.7262(4)	16.6403(5)	18.0605(2)	20.4100(3)
α (°)	90	90	90	90
β (°)	101.147(2)	109.771(1)	107.932(1)	90
γ (°)	90	90	90	90
Volume (Å^3)	5771.6(2)	2076.5(1)	5285.1(1)	2847.74(8)
Z	4	4	8	4
D_{calc} (g/cm^3)	1.857	1.805	1.513	1.762
Temperature (K)	173(2)	188(2)	173(2)	173(2)
$\mu_{Mo\ K\alpha}$ (cm^{-1})	7.859	7.174	4.499	5.623
$2\theta_{max}$ (°)	24.71	29.13	27.00	26.99
Crystal size (mm)	0.05 × 0.09 × 0.13	0.06 × 0.08 × 0.15	0.17 × 0.21 × 0.25	0.05 × 0.10 × 0.13
Index range	$-18 \leqslant h \leqslant 18$, $-22 \leqslant k \leqslant 21$, $-23 \leqslant l \leqslant 22$	$-17 \leqslant h \leqslant 17$, $-14 \leqslant k \leqslant 12$, $-22 \leqslant l \leqslant 22$	$-19 \leqslant h \leqslant 20$, $-23 \leqslant k \leqslant 24$, $-23 \leqslant l \leqslant 23$	$-14 \leqslant h \leqslant 13$, $-15 \leqslant k \leqslant 16$, $-26 \leqslant l \leqslant 23$
Number of reflections collected/observed	17 356	9883	18 275	15 131
Number of independent reflections	9760 (R_{int} = 0.0512)	5507 (R_{int} = 0.0451)	5762 (R_{int} = 0.0314)	6056 (R_{int} = 0.0674)
Number of observed reflections	6855	4031	4547	4414
Parameters	686	325	267	356
R_1 ($F_o > 2\sigma F_o$)	0.0476	0.0395	0.0245	0.0374
wR_2 (all data)	0.0930	0.0867	0.0573	0.0711
Goodness of fit (S)	1.081	1.057	1.028	0.964

tion from a concentrated Et_2O solution layered with pentane at −20 °C.

Low temperature (−100 °C for **1**, **3** and **6**, and −85 °C for **2**) diffraction data for all the crystals were collected on an Enraf–Nonius KappaCCD diffractometer [20] using graphite monochromated Mo Kα radiation ($\lambda = 0.71073$ Å). All the data sets were scaled, reduced and corrected for Lorentz and polarisation effects using DENZO-SMN [21]. The structures of **1** and **6** were solved with direct methods and refined anisotropically for all the non-hydrogen atoms, except those mentioned below, by full-matrix least squares calculations on F^2. Dynamic disorder of the C(3)–O(3) and C(4)–O(4) CO ligands in the structure of **1** prevented the anisotropic refinement of the C(3) and C(4) atomic positions.

The structures of **2** and **3** were solved by the interpretation of Patterson syntheses, which yielded the positions of the metal atoms. The structures were completed by full-matrix least squares calculations (SHELXL-97) [22] on F^2 and, unless stated otherwise, refined anisotropically.

Extensive disorder, in the form of a complete molecule of **2** orientated as a mirror image across a plane through C1 and C11, was found in the crystal structure of **2**. The low site occupancy of the minor disorder component [14.2(1)%] meant that it could only be refined isotropically and that the phenyl ring carbon atom positions had to be restrained to idealised 6-membered rings. In addition, the C(1b) atom was restrained to a reasonable position by fixing the Au–C(1b) and C(1b)–C(11b) bond lengths to sensible values.

Hydrogen atoms, with the exception of the imine hydrogen atom in the structure of **6**, were placed in idealised positions with their displacement parameters fixed at 1.5 times (for aliphatic hydrogen atoms) or 1.2 times (for aromatic hydrogen atoms) the equivalent isotropic displacement parameters of their parent atoms. The aforementioned hydrogen atom in **6** was located on the difference Fourier map and refined isotropically.

All calculations were performed using SHELX-97 [22] in the X-SEED [23] environment. ORTEP-III for Windows [24] was used to generate the various figures at the 50% probability level.

3. Results and discussion

3.1. Acyl gold compounds

Attempted syntheses of acyl gold compounds by reaction of Ph_3PAuCl and freshly prepared lithium acetyl/benzoyl pentacarbonyl chromates and tungstates were unsuccessful. Although evidence from IR analysis of the product mixtures pointed to weak acylgold–oxygen coordination to the $M(CO)_5$ fragments, the coordination could not be proven beyond all reasonable doubt. Furthermore, decomposition of the complexes – indicated by rapid darkening of the reaction mixtures – was frequently observed during the purification procedure. One such product, however, crystallised in moderate yield, in the form of an unusual lithium complex of complexes and solvent (Scheme 2).

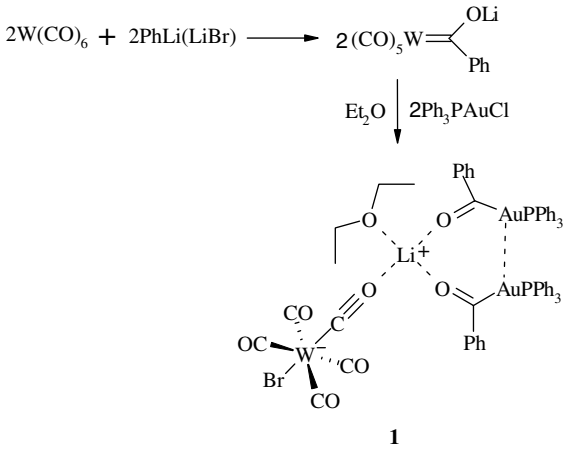

Scheme 2.

The formation of the tetrahedral lithium complex, **1**, is proposed to proceed as follows: LiBr, originally present in the freshly prepared PhLi solution employed to synthesise the lithium benzoylpentacarbonyl tungstate in the first step of the synthesis, reacts with expelled $W(CO)_5$ in the reaction mixture. The ionic species, $[BrW(CO)_5][Li]$, is formed, which precipitates, or rapidly crystallises, from the cooled (−20 °C) reaction mixture with two already-formed benzoyl-$AuPPh_3$ fragments and an Et_2O solvent molecule coordinated to the Li^+-cation.

A single crystal X-ray structure determination revealed this unexpected molecular structure for the product and also confirmed that the electrophilic addition of Ph_3PAu^+ to lithium acylpentacarbonyl tungstates indeed results in the formation of the acylgold(I) organyls.

The formation and precipitation/crystallisation of **1** is driven by its poor solubility in Et_2O. Equilibria of halide salts and coordinatively unsaturated $M(CO)_5$ fragments are well known [25]. The fact that simple acylgold–$M(CO)_5$ complexes could not be isolated successfully in these reactions is thus probably as a result of the poor stabilisation that the $M(CO)_5$ fragments receive from the acylgold complex (or Et_2O solvent molecules) in the reaction mixture, as shown by the nature of the $W(CO)_5$ fragment in **1**. No precipitation or crystallisation of **1** could be achieved in the presence of thf.

The formation of LiBr adducts of $W(CO)_5$, observed in the crystal structure of **1**, indicated a method for the preparation of the first free acylgold(I) complex, benzoyl-$AuPPh_3$ (**2**) (Scheme 3). If, instead of lithium benzoylpentacarbonyl tungstate, tetrabutylammonium

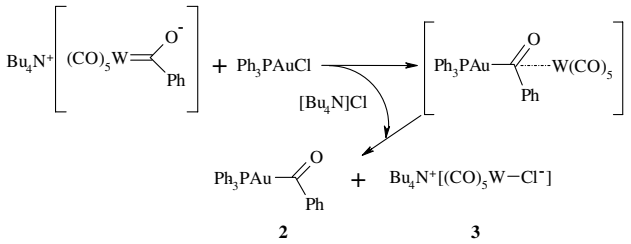

Scheme 3.

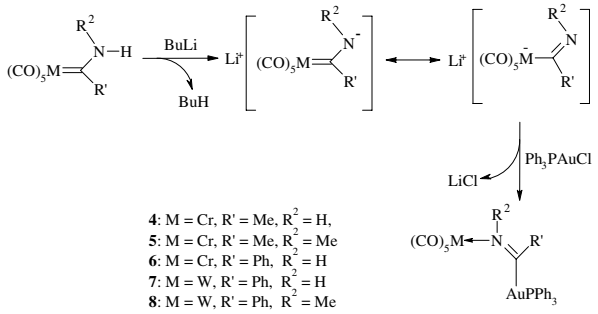

Scheme 4.

benzoylpentacarbonyl tungstate was employed as starting material, the reaction with Ph_3PAuCl led to the formation of benzoyl-$AuPPh_3$, $[Bu_4N][Cl]$ and an unsaturated $W(CO)_5$ fragment. The latter rapidly reacted with the $[Bu_4N][Cl]$ to yield the ionic species, $[ClW(CO)_5]$-$[Bu_4N]$ (**3**), which is sparingly soluble in Et_2O and rapidly precipitates from the cooled (0 °C) reaction mixture. Since the Bu_4N^+-cation in **3** cannot accommodate acyl coordination, as is observed for the Li-cation in the crystal structure of **1**, the free benzoyl-$AuPPh_3$ complex (**2**) remains in solution and can be isolated in high (72%) yields by crystallisation from concentrated Et_2O solutions. X-ray diffraction studies unequivocally confirmed the formation of both **2** and **3** in this reaction.

The mechanism involved in the formation of **1** and **2** is not clear. For their reaction, Haupt and co-workers [11] suggested a concerted mechanism in which a hypothetical ion pair complex, $[Re_2\{\mu\text{-}PPh_2\}_2(CO)_7\{C(O)R\}]^-[AuPPh_3]^+$, is converted to the acylgold(I)-coordinated rhenium complexes via an assumed bimetallic η^2-acyl transition state. The thermodynamic considerations they rely on are, however, not valid in the present situation.

Fischer, Schubert and Sarkar have reported the rearrangement of certain Fischer-type carbene complexes to ketones or aldehydes upon thermolysis [26]. In a recent paper, Sarkar and co-workers [27] suggests a probable mechanism for such a reaction involving electrophilic addition of a carbon electrophile onto the metal moiety, followed by a formal reductive elimination of a ketone fragment.

Based on these reports, a mechanism related to the aurolysis of deprotonated carbene complexes by Ph_3PAu^+ [10] should also be considered; W–Au interaction, for example, could occur prior to acylgold formation.

3.2. Imidoyl complexes of gold

The syntheses of complexes **4**–**8** (Scheme 4) were carried out by irreversible N-deprotonation of the respective group 6 metal aminocarbene complexes with 1 mol equiv. *n*-butyllithium at −78°C, followed by the addition of 1 mol equiv. Ph_3PAuCl to the reaction mixture. After addition of the Ph_3PAuCl, the reaction mixture was allowed to slowly warm up to room temperature over a period of 3 h. Removal of the solvent in vacuo yielded dark-yellow oily residues containing **4**–**8** (32–85% yields after separation). Separation of the complexes was carried out by low temperature (−15 °C) silica gel column chromatography with hexane/diethyl ether (2:1) as eluant, followed by crystallisation from a diethyl ether solution layered with pentane at −20 °C.

The novel formation of the {acetimidoyl-$AuPPh_3$}$M(CO)_5$ and {benzimidoyl-$AuPPh_3$}$M(CO)_5$ complexes (Scheme 4), **4**–**8**, probably proceeds along a reaction path similar to that of **1** and **2**. Perhaps the term aurolysis can therefore also be applied to describe the current reaction. Furthermore, it is interesting to note that this conversion appears to be stereospecific, since only the *Z*-isomers of **4**–**8** were isolated.

Coordination of the acetimidoyl-$AuPPh_3$ and benzimidoyl-$AuPPh_3$ moieties to the $M(CO)_5$ fragments through the nitrogen atoms in **4**–**8** is much stronger than the potential oxygen coordination of M in {acyl-$AuPPh_3$}$M(CO)_5$ (**2**). This is reflected by the fact that **4**–**8** are, unlike their oxygen analogues, stable in all common laboratory solvents (under inert conditions), are not involved in any ligand substitution reactions with solvent molecules or halide salts, and can be successfully isolated by column chromatography (SiO_2). A single crystal X-ray structure of **6** confirms the unique molecular structure of these compounds.

The closest example of a similar conversion in the literature is the thermolysis reaction of Fischer-type aminocarbene complexes in the presence of CO, which also yields imines [28].

We have reported that a second deprotonation-auration reaction with complexes **4** and **6** yields a novel triangular Au_2Cr cluster compound with an extraordinarily short Au···Au separation (2.69 Å) as the only isolable product [29].

3.3. Spectroscopic characterisation

3.3.1. NMR spectroscopy

Since **1** is an ionic compound, it is unlikely that the Li-coordination found in the single crystal X-ray

structure will persist in solution. However, small variances in the NMR data of the acylgold fragments in **1** and **2**, most notably of the acyl carbon atom ^{13}C chemical shift (δ 203.3 in **1**, δ 198.1 in **2**), were observed, suggesting that a weak interaction between the $W(CO)_5$ species and the acylgold complex does occur. It is interesting to note that this resonance in **2** is a small doublet ($^2J_{P-C}$ = 6.0 Hz), whereas it manifests as a broadened singlet in the ^{13}C NMR spectrum of **1**. The acyl carbon resonance in **2** at δ 198.1 is comparable to a value of δ 192.0 for such an atom in benzaldehyde. This suggests that there is not much electron loss to the gold atom after auration. The spectroscopic analysis of **3** agrees with that reported previously [25].

The ^1H NMR spectra of **4**, **6** and **7** are characterised, in particular, by broad imine proton resonances between δ 8.89 and δ 10.05. These chemical shifts suggest a great deal of electron donation from the imine nitrogen atom to the $M(CO)_5$ fragments. ^1H and $^{13}C\{^1H\}$ resonances for the methyl groups on the imine nitrogen atoms in **5** and **8** are also found shifted downfield from their usual positions in examples of uncoordinated imines, at δ 3.24 and 32.0 (complex **5**), and δ 3.34 and 32.4 (complex **8**) [30].

A good indicator for the amount of electron donation from the imine groups to the $M(CO)_5$ fragments in **4**–**8** is the chemical shift of the C=N imine ^{13}C resonances. These appear as doublets ($^2J_{C-P}$ = 122.1–131.9 Hz) between δ 232.4 and 239.6 for **4**–**6** and **8**. Curiously this resonance in **7** appears in a similar region of the ^{13}C NMR spectrum (δ 238.4), but as a greatly broadened singlet. These resonances show that the imidoyl carbon atoms are substantially deshielded and do not exclude the possibility that they could have a carbene-type character.

^{13}C resonances of the Ph groups bonded to the C=N imine carbon atom in **6**–**8** are characterised by a downfield shifted signal (compared to the starting material) representing the *ipso* carbon atom of this ring (δ 149.1, 149.4 and 148.8). This signal is, furthermore, broadened as a result of weak $^3J_{C-P}$ coupling. The ^{13}C resonances for the methyl carbon atoms in this position in **4** and **5** are found at δ 42.1 and 49.4, as a broadened singlet and a doublet ($^3J_{P-C}$ = 9.3 Hz), respectively.

3.3.2. Infrared spectroscopy

The infrared (IR) spectra of **1** and **2** were recorded as KBr pellets from crystals. The spectrum of **1** exhibits six clearly separated absorption bands in the carbonyl region. These values are in good agreement with reported CO vibrational modes for the $BrW(CO)_5^-$-anion in $[BrW(CO)_5][R_4N]$ [2064 cm^{-1} (w, $A_1^{(1)}$), 1904 (st, E), 1868 ($A_1^{(2)}$)] [25], although the 'E' vibrational modes in **1** differ somewhat. The crystal structure of **1** shows that the $BrW(CO)_5$-anion is coordinated to a Li-cation through the CO ligand *trans* to the Br. Although the Li-coordination to O(5) (Fig. 1) seems to have little effect on the $A_1^{(2)}$ vibrational mode, it may be responsible for substantial distortion within the $W(CO)_4$ coordination plane because it brings the anion into closer proximity to the rest of the molecules (particularly the phenyl ring of one of the benzoyl-$AuPPh_3$ fragments in the structure) in the solid state. This is also apparent in the observation of a relatively strong B_1 absorption mode, which is only IR active upon distortion of the C_{4v} local symmetry in the $BrW(CO)_5$ moiety. Instead of the single twofold degenerate E-vibrational mode observed for the $BrW(CO)_5^-$-anion in the $[BrW(CO)_5][R_4N]$ compound, two non-degenerate, clearly separated

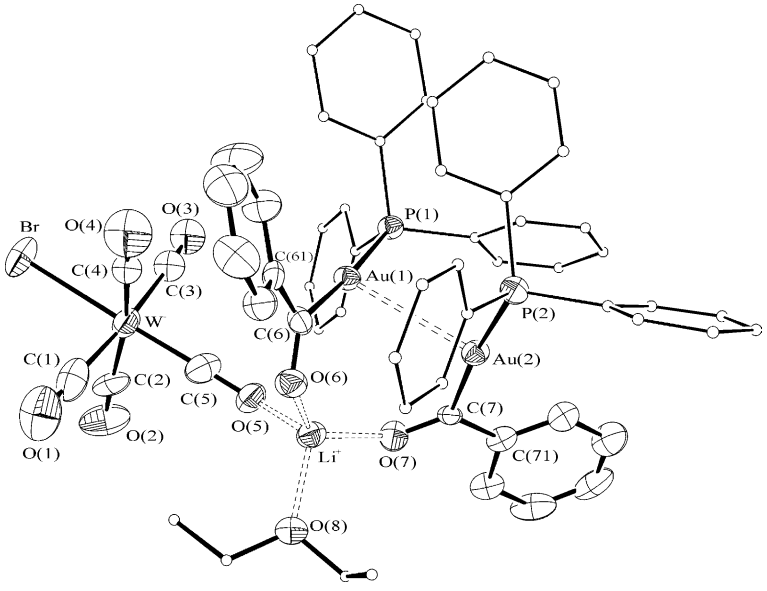

Fig. 1. ORTEP view of **1**, showing the numbering scheme (disordered CO and Et_2O atom positions, hydrogen atoms and anisotropic displacement parameters of carbon atoms of the PPh_3 group and Et_2O omitted for clarity). Displacement ellipsoids are shown at the 50% level.

vibrational modes are observed. Disorder found in the atomic positions of two CO ligands as well as the relatively long O(5)–Li separation in the crystal structure of **1** (possibly due to steric considerations), reported below, supports this interpretation of the IR data. The acyl C=O stretching frequency at 1560 cm^{-1} suggests a stronger acyl bond in **1** than in the literature reported Re-coordinated benzoyl-$AuPPh_3$ complex [υ(C=O) 1508 cm^{-1}].

The IR spectrum of **2** exhibits a single, medium intensity, CO stretching frequency (1606 cm^{-1}) situated next to two weaker $C{=}C_{conj}$ IR absorption modes (1588 and 1573 cm^{-1}). This result suggests, as would be expected for an uncoordinated benzoyl-$AuPPh_3$ moiety, substantially greater double bond character for the acyl C=O bond in **2** than in **1** and the Re-coordinated benzoyl-$AuPPh_3$ complex reported in the literature [11]. The crystal structure of **2**, reported below, confirms this suggestion as it reports the shortest C=O separation of the three compounds. The isolobal hydrogen analogue of complex **2**, benzaldehyde, exhibits a C=O stretching frequency at 1702 cm^{-1}, which suggests that there is either some measure of π-electron back-donation from the gold atom to the π*-orbital of the acyl carbon atom, or electron loss from the acyl carbon to the gold atom that weakens the C=O acyl bond in **2**.

The IR spectra of **4**–**8** were recorded as pentane solutions of the complexes in a NaCl cell. The IR spectra measured for these complexes each exhibit four clearly separated absorption bands in the carbonyl region, which represent the $A_1^{(1)}$, $A_1^{(2)}$, B_1 and E vibrational modes for molecules of the type $M(CO)_5L$. The C=N stretching frequency, expected to appear between 1500 and 1700 cm^{-1}, could, due to the presence of many $C{=}C_{conj}$ vibrational modes in the same region, unfortunately not be unambiguously identified in the IR spectra of these compounds.

3.3.3. Mass spectroscopy

FAB-mass spectra of **1**–**8** were characterised by high intensity peaks for PPh_3Au^+ and $(PPh_3)_2Au^+$ fragments, the latter being an artifact of the analytical method. Molecular ions could be identified for **2**, **4** and **6**, while for **7** the fragment M-2CO was found. Peaks corresponding to free benzoyl-$AuPPh_3$ and some WBr species were identified in the FAB-mass spectrum of **1**.

3.4. X-ray structure determinations

The low temperature crystal and molecular structures of **1** (173 K), **2** (173 K), **3** (188 K) and **6** (173 K) (Figs. 1, 3–5) were determined by X-ray diffraction techniques. Selected bond lengths and angles for **1**, **2**, **3** and **6** are listed in Table 2.

The molecular structure of **1** (Fig. 1) revealed a novel electrostatically associated ionic structure for this compound. It consists of a Li-cation that is roughly tetrahedrally coordinated to an Et_2O molecule, a $BrW(CO)_5$-anion and two benzoyl-$AuPPh_3$ complexes. Coordination of the Li-cation to the $BrW(CO)_5$ anion is through the oxygen atom of the CO ligand *trans* to the Br atom, while coordination to the two benzoyl-$AuPPh_3$ complexes is through the oxygen atoms of the acyl moieties. The benzoyl-$AuPPh_3$ complexes are, furthermore, linked to each other by weak aurophilic Au–Au interactions [Au(1)···Au(2) = 3.1213(5) Å] with a torsion angle [C(6)–Au(1)–Au(2)–C(7)] of 103.0(4)° between the two pseudo-linear Au(I) coordination modes. C(6)–Au(1)–P(1) and C(7)–Au(2)–P(2) angles of 175.6(3)° and 172.5(3)° describe how the linear coordination mode of Au(I) is distorted towards the neighbouring gold atom due to the aforementioned aurophilic interactions. An intramolecular non-bonded face-to-edge phenyl-interaction, involving a phenyl ring from each PPh_3 group in the benzoyl-$AuPPh_3$ moieties [C(13X) and C(22X) rings], further stabilises the Au–Au linked configuration.

The tetrahedral coordination of the Li-cation is somewhat distorted from the ideal, with the largest angle between two of the coordinating oxygen atoms being 124.2(9)° [O(6)–Li–O(7)] between the oxygen atoms of the two coordinating benzoyl-$AuPPh_3$ complexes. The $BrW(CO)_5$-anion exhibits dynamic disorder (not shown in Fig. 1) in the positions of two of its CO ligands [C(3)–O(3) and C(4)–O(4)]. This could be partially modelled by two different positions for these CO groups identified from the difference Fourier map with site occupancies of

Table 2
Selected bond lengths (Å) and angles (°)

Compound	1	2	3	6
Au–P	2.312(3), 2.317(3)	2.313(1)		2.301(2)
Au–C_{sp2}	2.046(10), 2.079(9)	2.085(5)		2.034(7)
C_{sp2}–O/N	1.238(11), 1.234(10)	1.200(7)		1.281(9)
Au...Au	3.1213(5)			
W/Cr–Br/Cl	2.6913(12)		2.5602(8)	
W/Cr–C_{trans}	1.909(12)		1.939(4)	1.853(8)
W/Cr–C_{cis} (average)	2.01(2)		2.033(4)	1.898(9)
C_{sp2}–Au–P	175.6(3), 172.5(3)	176.4(1)		171.2(2)
Au–C_{sp2}–O/N	122.3(8), 121.1(7)	123.4(4)		124.2(6)

0.63:0.37. Elongated anisotropic displacement parameters on O(3) and O(4) [C(3) and C(4) could not be anisotropically refined] indicated the presence of the dynamic disorder. A small degree of dynamic disorder (not shown in Fig. 1) in the ethyl groups of the Et_2O molecule, as indicated by enlarged anisotropic displacement parameters for the atoms involved, is also observed.

The reason for this disorder can be seen in the packing of **1** (Fig. 2), where the molecules pack in regular rows in a structure that leaves two open channels parallel to the *b*-axis per unit cell. Both the disordered CO ligands and the Li-coordinated Et_2O solvent molecules border directly on these channels, allowing freedom of movement of these groups within the crystal lattice. Furthermore, rapid crystal degradation was observed upon isolation of the crystalline mass of **1** and is ascribed to the loss of Et_2O from the crystal lattice along these channels.

The crystal and molecular structure of the free benzoyl-$AuPPh_3$ complex, **2** (Fig. 3), represents the first example of its kind.

The Au(1a)–C(1a) bond [2.085(5) Å] in **2** is within the expected range for Au(I)–C(sp^2) single bonds [31]. The

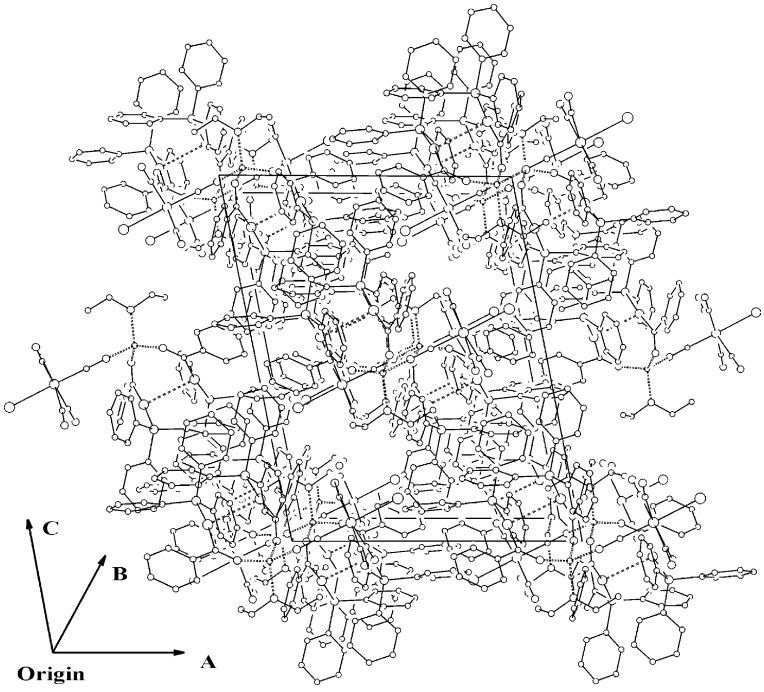

Fig. 2. Packing diagram of **1**, viewed along the *b*-axis of the unit cell showing the channels and the positions of the Et_2O molecules and disordered CO ligands within the unit cell.

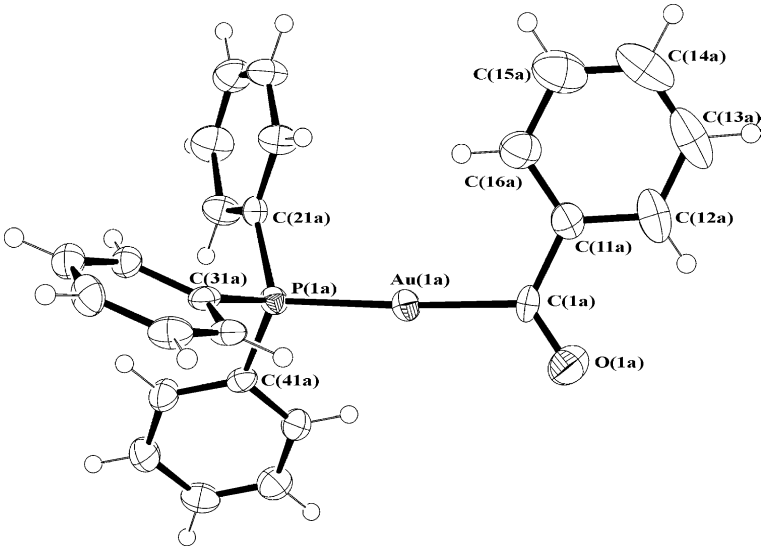

Fig. 3. ORTEP view of **2** (a-orientation with 85.8% site occupancy), showing the numbering scheme. Displacement ellipsoids are shown at the 50% level.

Au(1a)–P(1a) bond [2.313(1) Å] is also normal [11,32]. O(1a) is unmistakably double bonded to the acyl carbon atom [C(1a)–O(1a) = 1.200(7) Å]. This bond is also, as would be expected, slightly shorter than the corresponding Li-coordinated and Re-coordinated C=O bonds in the structures of **1** and the only other structurally characterised acylgold(I) adduct referred to above [11]. The sp^2 hybridisation of C(1a) is confirmed by its nearly perfectly flat bonding geometry [the greatest deviation from the least-squares plane defined by Au(1a), C(1a), O(1a), C(11a) is 0.012(4) Å for C(1a)]. Despite the fact that no intermolecular metal–metal interactions are observed in the crystal structure of **2**, the P(1a)–Au(1a)–C(1a) angle deviates from 180° [P(1a)–Au(1a)–C(1a) = 176.4(1)°]. This is most likely due to packing effects, since the acyl oxygen atom, O(1a), is situated close to one of the phenyl rings of the PPh_3 group of a neighbouring molecule. The other two phenyl rings are involved with face-to-edge π interactions with neighbouring molecules.

The crystal and molecular structure of $[ClW(CO)_5][Bu_4N]$ (**3**), which precipitated from the same reaction mixture as **2**, is shown in Fig. 4. Although **3** is a well-known and stable organometallic compound and has often been applied as starting material in reaction sequences [25], its crystal structure has not yet been reported. Bond lengths and angles within the $W(CO)_5Cl$-anionic and the Bu_4N-cationic components of **3** are normal for such moieties [33]. A W–C(4) separation of 1.939(4) Å, which is ~0.1Å shorter than the other W–C distances in the structure, shows the influence of the weaker (compared to CO) *trans* directing chlorine ligand.

Compound **3** exhibits an efficient packing arrangement that probably aids its crystallisation from the reaction mixture. Layers of cations and anions are closely packed, roughly parallel to the *a*-axis, with no solvent-accessible or other significant voids or channels present.

The structure of **6** (Fig. 5) clearly exhibits a benzimidoyl-$AuPPh_3$ moiety coordinated through its imine nitrogen atom to a $Cr(CO)_5$ group and demonstrates that it is the *Z*-isomer that forms. Compound **6** is the first organoimidoyl complex of gold for which the crystal and molecular structures have been determined. This complex, furthermore, acts as a neutral N-donor ligand to a $Cr(CO)_5$ fragment, thereby also being the first example of a bimetallic imidoylgold(I) complex that is coordinated through the imine nitrogen atom to a metal other than gold.

The Au–C(1) bond length in **6** [2.034(7) Å] is typical for an Au(I)–C(sp^2) σ-bond [31]. The C(1)–N separation [1.281(9) Å] confirms the double bond character of this bond. There is a near planar bonding geometry around C(1) [deviations from the least squares plane calculated through C(1), Au, C(41) and N are 0.024(5), 0.006(1), 0.008(2) and 0.010(2) Å, respectively].

Deviations from planarity of the least squares plane through Cr, C(2), C(3), C(4) and C(5) of 0.045(3), −0.077(4), 0.055(4), −0.075(4) and 0.052(4) Å describe its distortion due to the coordination of the sterically large benzimidoyl-$AuPPh_3$ moiety. A small Au–C(1)–Cr–C(2) torsion angle of 13.3(5)° shows that the Au–C(1) bond is surprisingly close to parallel to the Cr–C(2) bond. This is also reflected in the 170.3(6)° and 171.2(2)° Cr–C(2)–O(2) and P–Au–C(1) angles that are distorted from linearity (vide infra).

The position of the imine hydrogen atom (H) could be determined from the difference Fourier map and refined isotropically. This hydrogen atom position is distorted toward the $Cr(CO)_5$ fragment, as can be seen in the C(1)–N–H and Cr–N–H angles [127(6)° and 96(6)°] and the short Cr–H separation [2.35(8) Å].

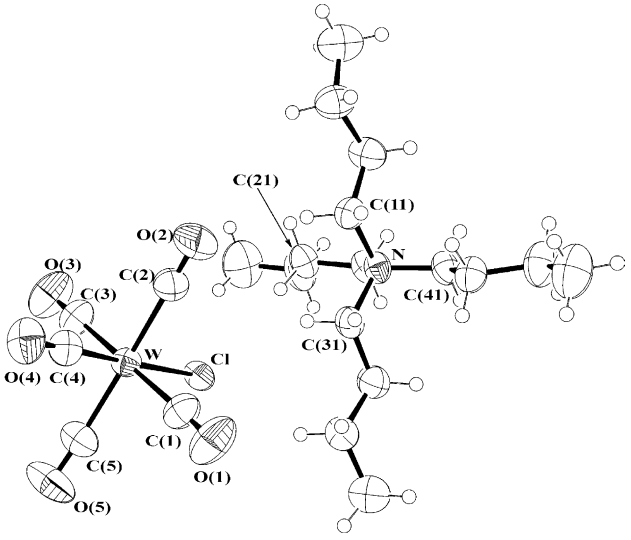

Fig. 4. ORTEP view of **3**, showing the numbering scheme. Displacement ellipsoids are shown at the 50% level.

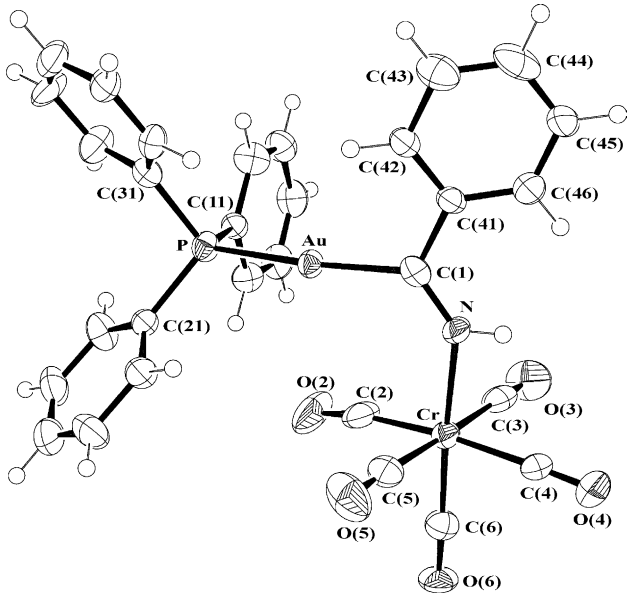

Fig. 5. ORTEP view of **6**, showing the numbering scheme. Displacement ellipsoids are shown at the 50% level.

Short non-bonded intermolecular interactions between molecules of **6** occur along the *a*-axis of the unit cell, involving the oxygen atom [O(6)] of the CO ligand *trans* to the imine coordination, a hydrogen atom from the benzimidoyl ring [H(43)] and a hydrogen atom from a phenyl ring in the PPh_3 group [H(33)]. It is likely that this interaction and an offset herringbone packing configuration of the P–Au–C(1) bonds are also partly responsible for the high degree of distortion from the usually linear P–Au–C(1) coordination mode.

4. Conclusions

In this paper, we have described how formally deprotonated pentacarbonyl(group 6)hydroxy- and aminocarbene (alternatively, acyl and imidoyl) complexes may function as synthons in transmetallation for the preparation of unprecedented free acyl and $(CO)_5$M-N-coordinated (M = Cr, W) imidoyl compounds of gold. The mechanism of these reactions is not known, but metal–metal (group 6···Au) interactions deserve consideration. It is clear, however, that acyl complexes of gold do not form by CO-insertion into the gold–carbon single bond. In the presence of other acidic and basic units, the gold acyl complex engages in various forms of intramolecular interaction in the solid state. The crystal and molecular structures of a well-known member of the $(CO)_5MX^-$ family, $[(CO)_5WCl]NBu_4$, have also been determined.

Acknowledgements

We thank the NRF, the Volkswagen-Stiftung and the University of Stellenbosch for financial support.

Appendix A. Supplementary data

Crystallographic data for the structural analysis have been deposited with the Cambridge Crystallographic Data Centre, CCDC Nos. 263482 (**1**), 263483 (**2**), 263484 (**3**) and 263485 (**6**). Copies of this information may be obtainded free of charge from the Director, CCDC, 12 Union Road, Cambridge, CB2 1E2, UK (fax: +44-1223-336-033; e-mail: deposit@ccdc.ca.ac.uk, www: http://www.ccdc.cam.ac.uk). Supplementary data associated with this article can be found, in the online version, at doi:10.1016/j.ica.2005.03.029.

References

[1] (a) G.E. Coates, M.L.H. Green, K. Wade, Organometallic compounds, Methuen, London, 1968, p. 257;
(b) A. Wojcicki, Adv. Organomet. Chem. 11 (1973) 87;
(c) F. Calderazzo, Angew. Chem., Int. Ed. Engl. 16 (1977) 299;
(d) E.J. Kuhlman, J.J. Alexander, Coord. Chem. Rev. 33 (1980) 195;
(e) J.P. Collman, L.S. Hegedus, J.R. Norton, R.G. Finke, Principles and Applications of Organotransition Metal Chemistry, second ed., University Science Books, Mill Valley, CA, 1980, p. 619.
[2] (a) L.D. Durfee, I.P. Rithwell, Chem. Rev. 88 (1988) 1059;
(b) A.R. Cutler, P.K. Hanna, J.C. Vites, Chem. Rev. 88 (1988) 1363;
(c) T. Kinnunen, K.J. Laason, Organomet. Chem. 628 (2001) 222.
[3] J.R. Moss, J. Mol. Catal. A: Chem. 107 (1996) 169.
[4] M.E. Dry, Catal. Today 6 (1990) 183.
[5] (a) E.O. Fischer, A. Maasböl, Angew. Chem., Int. Ed. Engl. 3 (1964) 580;
(b) E.O. Fischer, A. Maasböl, Chem. Ber. 100 (1967) 2445.
[6] M.F. Semmelhack, G.R. Lee, Organometallics 6 (1987) 1839.
[7] (a) See for example: J.A. Van Doorn, C. Masters, H.C. Volger, J. Organomet. Chem. 105 (1976) 245;
(b) J.A. Gladysz, J.C. Selover, C.E. Strouse, J. Am. Chem. Soc. 100 (1978) 6766;
(c) E.O. Fischer, Adv. Organomet. Chem. 14 (1976) 1.
[8] (a) J.E. Ellis, J. Organomet. Chem. 86 (1975) 1;
(b) R.B. King, Acc. Chem Res. 3 (1970) 417.
[9] S. Komiya, T. Sone, S. Ozaki, M. Ishikawa, N.J. Kasuga, Organomet. Chem. 428 (1992) 303.
[10] H.G. Raubenheimer, M.W. Esterhuysen, A. Timoshkin, Y. Chen, G. Frenking, Organometallics 21 (2002) 3173.
[11] H.-J. Haupt, D. Petters, U. Flörke, J. Organomet. Chem. 553 (1998) 497.
[12] M.W. Esterhuysen, H.G. Raubenheimer, Eur. J. Inorg. Chem. (2003) 3061.
[13] N. Luruli, V. Grumel, R. Brüll, A. duToit, H.G. Raubenheimer, J. Polym. Sci., Part A: Polym. Chem. 42 (2004) 5121.
[14] (a) A. Burini, R. Bravi, J.P. Fackler Jr., R. Galassi, T.A. Grant, M.A. Omary, B.R. Pietroni, R.J. Staples, Inorg. Chem. 39 (2000) 3158;
(b) W.P. Fehlhammer, L.F. Dahl, J. Am. Chem. Soc. 94 (1972) 3370;
(c) H.G. Raubenheimer, F. Scott, G.J. Kruger, J.G. Toerien, J.R. Otte, W. van Zyl, T. Taljaard, P.J. Olivier, L. Linford, J. Chem. Soc., Dalton Trans. (1994) 2091;
(d) H.G. Raubenheimer, P.J. Olivier, L. Lindeque, M. Desmet, J. Hrusak, G.J. Kruger, J. Organomet. Chem. 544 (1997) 91;
(e) K.M. Lee, C.K. Lee, I.J.B. Lin, Angew. Chem., Int. Ed. Engl. 36 (1997) 1850.
[15] (a) A.L. Balch, M.M. Olmstead, J.C. Vickery, Inorg. Chem. 38 (1999) 3494;
(b) M. Lanfranchi, M.A. Pellinghelli, A. Tiripicchio, F. Bonati, Acta Crystallogr., Sect. C (Cr. Str. Comm.) 41 (1985) 52;
(c) A. Tiripicchio, M. Camelini, G. Minghetti, J. Organomet. Chem. 171 (1979) 399;
(d) J.C. Vickery, A.L. Balch, Inorg. Chem. 36 (1997) 5978.
[16] M.R. Winkle, J.M. Lansinger, R.C. Roland, J. Chem. Soc., Chem. Commun. (1980) 87.
[17] J.P. Fackler Jr., Inorg. Synth. 21 (1982) 325.
[18] (a) L.S. Hegedus, M.A. McGuire, L.M. Schultz, Org. Synth. 65 (1987) 140;
(b) E.O. Fischer, A. Maasböl, Chem. Ber. 100 (1967) 2445.
[19] E.O. Fischer, M. Leupold, Chem. Ber. 105 (1972) 599.
[20] COLLECT, Data Collection Software, Nonius BV Delft, The Netherlands, 1998.
[21] Z. Otwinowski, W. Minor, Method Enzymol. 276 (1997) 307.
[22] G.M. Sheldrick, SHELX SHELX-97. Program for Crystal Structure Analysis, University of Göttingen, Germany, 1997.
[23] L.J. Barbour, J. Supramol. Chem. 1 (2001) 189.
[24] L.J. Farrugia, J. Appl. Cryst. 30 (1997) 565.

[25] J.L. Atwood, S.G. Bott, J.C. Junk, M.T. May, J. Organomet. Chem. 487 (1995) 7, and references therein.
[26] (a) E.O. Fischer, U. Schubert, J. Organomet. Chem. 170 (1979) C13; (b) U. Schubert, H. Hörnig, J. Organomet. Chem. 273 (1984) C11; (c) M. Nandi, K.M. Sathe, A. Sarkar, J. Chem. Soc., Chem. Commun. (1992) 793.
[27] K.M. Sathe, M. Nandi, S.R. Amin, V.G. Puranik, A. Sarkar, Organometallics 15 (1996) 2881.
[28] J.A. Connor, P.D. Rose, J. Organomet. Chem. 46 (1972) 329.
[29] M.W. Esterhuysen, H.G. Raubenheimer, Acta Crystallogr. Sect. C. 59 (2003) m286.
[30] J.-J. Brunet, A. Capperrucci, R. Chauvin, Organometallics 15 (1996) 5254.
[31] (a) H.G. Raubenheimer, G.J. Kruger, C.F. Marais, J.T.Z. Hattingh, L. Linford, P.H. van Rooyen, J. Organomet. Chem. 355 (1988) 337;
(b) H.G. Raubenheimer, M. Desmet, G.J. Kruger, J. Chem. Soc., Dalton Trans. (1995) 2067.
[32] (a) P.G. Jones, Gold Bull. 14 (1981) 102, 159;
(b) P.G. Jones, Gold Bull. 16 (1983) 114;
(c) P.G. Jones, Gold Bull. 19 (1986) 46.
[33] C. Burschka, W.A. Schenk, Z. Anorg. Allg. Chem. 477 (1981) 149.